Inorganica Chimica Acta, 9 (1974) 183–188

The Photolysis of Trioxalatogermanate(IV) in Aqueous Solution*. II. Kinetics and Mechanism

E. L. J. BREET and R. van ELDIK
Research Unit for Chemical Kinetics, Potchefstroom University for C.H.E., Potchefstroom, Republic of South Africa
Received September 19, 1973

The photolysis of the trioxalatogermanate(IV) ion has been investigated kinetically in an effort to solve the problems arising from a previous investigation. The decomposition rate has been measured spectrophotometrically in terms of the rate of formation of the photolysis product, which shows a distinctive absorption in the charge transfer region. The principal feature of the proposed photolysis mechanism is the photoactivation of the bioxalate ion, which subsequently interacts with the oxyoxalatogermanate(IV) ion to produce a divalent germanium oxalato compound as photolysis product.

Introduction

Reaction kinetics have been used successfully to reveal the mechanism of the photochemical and/or thermal decomposition of various metal oxalato complexes. A few representative examples include the decomposition of the complex ions $Fe(C_2O_4)_3^{3-}$ (ref. 1), $Cu(C_2O_4)_2^{2-}$ (ref. 2) and $Hg(C_2O_4)_2^{2-}$ (ref. 3). In the majority of cases the metal ion is reduced while the oxalate ligand is oxidised to carbon dioxide.

In our previous paper[4] on the photochemical behaviour of the trioxalatogermanate(IV) ion, the conclusion was drawn that the decomposition products are mainly carbon dioxide and a divalent germanium oxalato compound, the yield of which depends on a preequilibration prior to irradiation. A kinetic analysis of the photolysis has been adopted for the present investigation, attempting to throw light on the reaction mechanism.

Experimental

The same experimental and analytical instruments described in our previous paper concerning this investigation have been applied. The test solutions, comprising weighed amounts of complex in suitable oxalate buffers, were not sensitized for reasons previously outlined.[4]

Results and Discussion

The presentation of the experimental results is simplified by using the following symbols:

[X]	complex ion concentration (mol liter^{-1})
$[Ox]_T$	total oxalate concentration (mol liter^{-1})
$[H^+]$	hydrogen ion concentration (mol liter^{-1})
μ	ionic strength (mol liter^{-1})
I	irradiation intensity
d	slitwidth (cm)
T	temperature (K)
A	spectrophotometric absorbance of photolysis product
t	irradiation time (min)
R_o	overall observed reaction rate
R	initial reaction rate
k_o	overall observed rate constant
k	initial rate constant

The kinetic analysis was effected by measuring A at 294 nm as a function of t for each of six rate parameters. These were varied individually, maintaining the remaining parameters at a constant value of $[X] = 1.5 \times 10^{-2}$; $[Ox]_T = 3.0 \times 10^{-2}$; pH = 2.8; $\mu = 0.015$; d = 0.95; T = 287. Since the results reflect the kinetics of the overall reaction

$$Ge^{IV} \underset{\Delta,\, k_{II}}{\overset{h\nu,\, k_I}{\rightleftharpoons}} Ge^{II}$$

the analysis of the photochemical forward reaction requires utilization of initial rate data to exclude the effect of the thermal reverse reaction. The initial reaction rate R is given by dA/dt rather than by dc/dt since the molar extinction coefficient is unknown for the photolysis product which has not yet been isolated. It is calculated as $\Delta A/\Delta t$ for small Δt values within

* Presented at the 22nd Convention of the S.A. Chemical Institute, Pretoria, July 1972.

the first hour of irradiation when the effect of the thermal reverse reaction is minimal.

The chemical rate parameters are the concentration variables [X], $[Ox]_T$ and $[H^+]$.

TABLE I. [X] as Rate Parameter.

t	A at 294 nm			
	$[X] \times 10^2$			
	0.5	1.0	1.5	2.0
30	0.10	0.16	0.23	0.22
60	0.30	0.40	0.51	0.53
90	0.34	0.49	0.68	0.84
120	0.36	0.54	0.73	1.02
150	0.41	0.60	0.78	1.13

The results for [X] as rate parameter are presented in Table I. From Figure 1 the infinity absorbance A_∞ for each [X] is obtained by graphical extrapolation and checked by calculating the corresponding value from a computer fitted curve equation. Plots of log $(A_\infty - A_t)$ versus t, A_t being the absorbance at time t, are shown in Figure 2. The observed rate constants summarized in Table II indicate that the overall reaction obeys first-order kinetics. Thus $R_o = k_o[X]$, the average value of $k_o = k_I + k_{II}$ being 0.97×10^{-2} min^{-1}.

The relation between R and [X] is shown in Figure 3. The equation

$$R = k_1[X] \quad (1)$$

mathematically describes the linear relation, indicating that the photolysis is first-order with respect to [X].

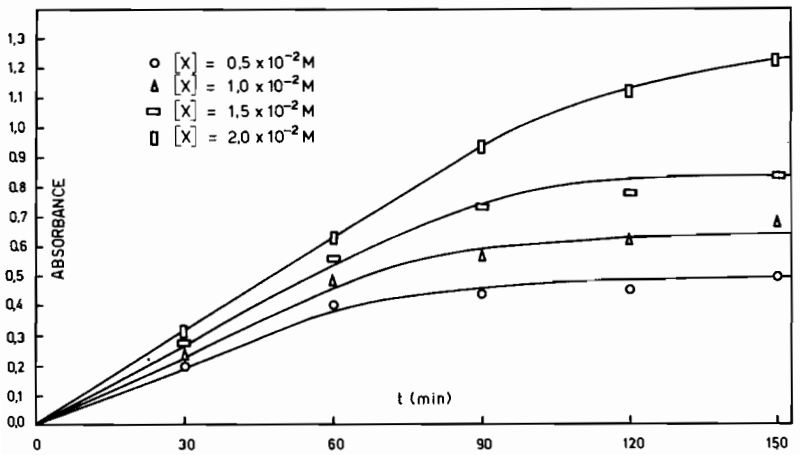

Figure 1. [X] as rate parameter.

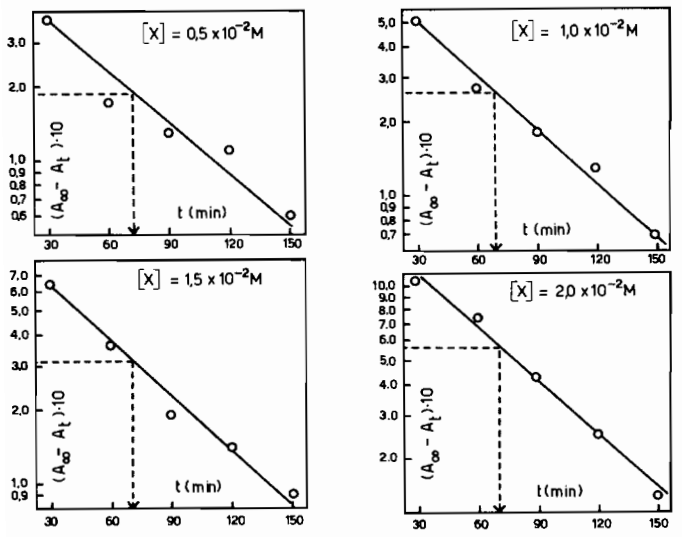

Figure 2. k_o for various [X].

TABLE II. k_o for Various [X].

$[X] \times 10^2$	A_∞	$t_{1/2}$	$k_o \times 10^2$
0.5	0.47	73	0.95
1.0	0.67	71	0.98
1.5	0.87	72	0.96
2.0	1.27	71	0.98

TABLE III. k_o for Various $[H^+]$.

pH	A_∞	$t_{1/2}$	$k_o \times 10^2$
1.65	0.45	75	0.92
2.15	0.70	77	0.90
2.80	0.93	72	0.96
3.65	0.87	71	0.98

It is evident from the same figure that R is independent of $[Ox]_T$ as long as oxalate is present. The overall observed rate constants for the various $[Ox]_T$ are calculated as before, the average value 0.97×10^{-2} min^{-1} for k_o being identical with that obtained in Table II.

The overall observed rate constants for the various $[H^+]$ are presented in Table III. The average value 0.94×10^{-2} min^{-1} for k_o is in good agreement with the values calculated above.

It is evident from Figure 4 that R increases linearly with pH to a maximum above pH 3. When 1/R is plotted *versus* $[H^+]$, a straight line with slope $k_A \sim 10^4$ and intercept $k_B \sim 10^2$ is obtained, enabling the results to be mathematically described by the equation

$$R = \frac{k_2}{[H^+] + k_3} \qquad (2)$$

with $k_2 = 1/k_A \sim 10^{-4}$ and $k_3 = k_B/k_A \sim 10^{-2}$. This indicates that the equation will show a linear $[H^+]$ dependence at low pH and an $[H^+]$ independence at high pH.

The calculation of the ion product for the overall reaction is accomplished by plotting $\log k_o$ versus $\mu^{1/2}$, the overall observed rate constants for the various μ being given in Table IV.

The ion product $Z_A A_B$ for the photochemical part of the overall reaction is calculated from the slope of the line $\log k = \log k_{\mu=0} + Z_A Z_B \mu^{1/2}$, k being calculated from equation (1). The value –2 obtained for $Z_A Z_B$ indicates participation of oppositely charged ions in the rate-determining step, but care is taken not to over-estimate the importance of this value for the disclosure of the photolysis mechanism since (i) the conclusion is drawn in literature[5] that the ionic strength relationship seems to be invalid for photoactivated species participating in the rate-determining step,

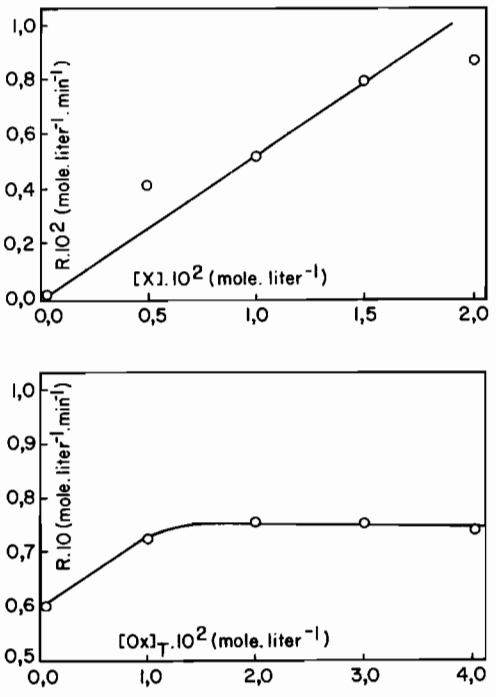

Figure 3. Influence of [X] and $[Ox]_T$ on R.

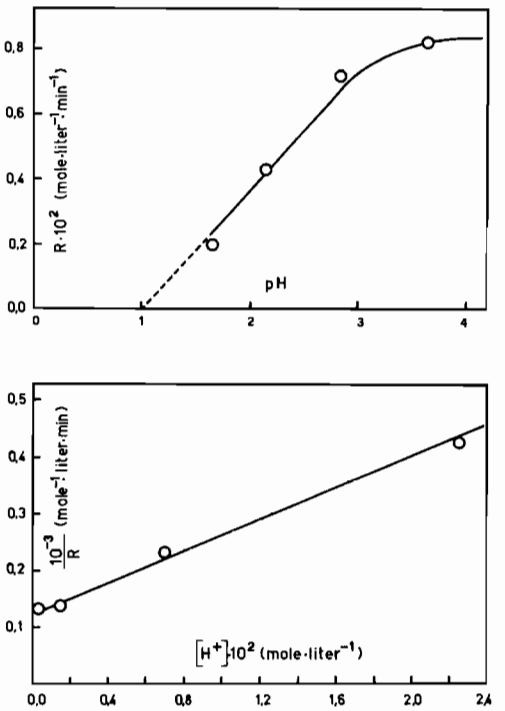

Figure 4. $[H^+]$ as rate parameter.

TABLE IV. k_o for Various μ.

μ	A_∞	$t_{1/2}$	$k_o \times 10^2$
0.105	1.21	70	0.99
0.145	1.08	76	0.91
0.185	0.87	83	0.84
0.225	0.70	90	0.77

TABLE VI. k_o for Various I.

d	A_∞	$t_{1/2}$	$k_o \times 10^2$
0.32	0.55	71	0.98
0.63	0.95	71	0.98
0.95	1.25	70	0.99
1.27	1.40	71	0.98

(ii) the decrease in the rate constant may be attributed to a "scavenging effect" of the medium adjusting the ionic strength (KCl) on the photochemical radiation process and/or possible subsequent interaction between photoactivated species.

Experiments were performed to determine the influence of μ at the extreme pH values given in Table III. The ion product Z_AZ_B varies with pH to such a slight extent that it deserves no further discussion.

The overall observed rate constants for the various T in Table V enable the calculation of the activation energy for the overall reaction by plotting $\log k_o$ *versus* $^1/T$.

The rate constants calculated from initial rate data allow the activation energy ΔH^* for the photochemical part of the overall reaction to be calculated from the slope of the line $\log k = -\Delta H^*/2.3RT$ + constant. The small value $\Delta H^* \sim 20$ kJ mol^{-1} indicates that the rate-determining step is a secondary reaction which follows the primary photoactivation for which a greater energy demand exists.

The irradiation intensity I was controlled by varying slitwidth as described in the experimental section of the previous paper.[4] The results are summarized in Table VI, the average value 0.98×10^{-2} min^{-1} for k_o being in good agreement with the previously calculated values.

The straight line obtained by plotting R *versus* d is mathematically described by the equation

$$R = k_4 I \tag{3}$$

where k_4 is a proportionality constant.

It is concluded from the experimental results that the observed rate constant k_o is dependent on μ and T but independent of [X], $[Ox]_T$, $[H^+]$ and I, while the initial reaction rate R is dependent on [X], $[H^+]$, μ, I and T but independent of $[Ox]_T$ as long as oxalate is present. The experimental initial rate equation is obtained as

$$R = \frac{k'[X]I}{[H^+] + k''} \tag{4}$$

by combining equations (1), (2) and (3).

The proposed mechanism is based on the comprehensive explanation in our previous paper[4] why reactions (5) and (6) are assumed to occur during the preequilibration:

$$Ge(C_2O_4)_3^{2-} + H_2O \underset{\leftarrow k_{-5}}{\overset{k_5\rightarrow}{}} GeO(C_2O_4)_2^{2-} + H^+ + HC_2O_4^- \tag{5}$$

$$Ge(C_2O_4)_3^{2-} + OH^- \underset{\leftarrow k_{-6}}{\overset{k_6\rightarrow}{}} GeO(C_2O_4)_2^{2-} + HC_2O_4^- \tag{6}$$

Since no evidence exists that the complex ion GeO $(C_2O_4)_2^{2-}$ is primarily photoactivatable, it is assumed that in the pH range under consideration ($1.65 < pH < 3.65$) the bioxalate ion will be the main contributing photoactive spesies

$$HC_2O_4^- \xrightarrow[k_7, I]{h\nu} [HC_2O_4^-]^* \tag{7}$$

It was previously shown that the bioxalate and oxalate ions are much more photoactive than oxalic acid which hardly shows any photoactivity.[6] In high acidic solution ($pH < 1$) mainly oxalic acid is present, shifting the equilibria (5) and (6) to the left. This explains why nearly no photodecomposition is detected at high acidity (Figure 4). The fact that the presence of an oxalate buffer improves photoactivation (Part I, Figure 1[4]; Part II, Figure 3) supports the assumption that the bioxalate ion is the primary photoactivated species. In the absence of an oxalate buffer the bioxalate ions produced during the preequilibration (reactions (5) and (6)) will be responsible for the observed lower photoactivity. An increase in $[Ox]_T$ will increase $[HC_2O_4^-]$ but simultaneously decrease $[GeO(C_2O_4)_2^{2-}]$, thus explaining the independence of R with respect to $[Ox]_T$ (Figure 3).

The photochemical rate-determining step is reaction (8), implying energy transfer rather than thermal colli-

TABLE V. k_o for Various T.

T	$t_{1/2}$	$k_o \times 10^2$
287	85	0.82
296	74	0.94
305	69	1.00
314	60	1.15

sion in agreement with the low value of the activation energy.

$$GeO(C_2O_4)_2^{2-} + [HC_2O_4^-]^* \xrightarrow{k_8} Ge(C_2O_4)_2(OH)(C_2O_4^*)^{3-} \quad (8)$$

The value $Z_AZ_B = +2$ for the ions participating in reaction (8) can be made to agree with the experimentally obtained value $Z_AZ_B = -2$ (if applicable, in spite of the doubt thrown on its importance) by reasonably assuming "scavenging" participation of the chloride ion.

$$Ge(C_2O_4)_2(OH)(C_2O_4^*)^{3-} \xrightarrow[k_9]{} Ge(C_2O_4)_2^{2-} + 2CO_2 + OH^- \quad (9)$$

The decomposition reaction (9) leads to the reaction products. The production of carbon dioxide is in agreement with the radiochemical tracer results (Part I).[4] Although the structural characteristics of the divalent germanium species could not be revealed experimentally, it is reasonably assumed to be a simple or complex oxalate since no evidence for the presence of free Ge^{2+} ions in solution exists.[7]

The derivation of the theoretical initial rate equation is accomplished by applying the stationary state approximation to the preequilibrium to obtain a concentration expression for the $GeO(C_2O_4)_2^{2-}$ species.

$$\frac{d[GeO(C_2O_4)_2^{2-}]}{dt} = 0$$

$$= k_5[Ge(C_2O_4)_3^{2-}][H_2O] + k_6[Ge(C_2O_4)_3^{2-}][OH^-]$$

$$-k_{-5}[GeO(C_2O_4)_2^{2-}][H^+][HC_2O_4^-] - k_{-6}[GeO(C_2O_4)_2^{2-}][HC_2O_4^-]$$

or

$$[GeO(C_2O_4)_2^{2-}] = \frac{\{k_5[H_2O] + k_6[OH^-]\}[Ge(C_2O_4)_3^{2-}]}{\{k_{-5}[H^+] + k_{-6}\}[HC_2O_4^-]}$$

The approximation $k_5[H_2O] \gg k_6[OH^-]$ for the pH range in which experiments were performed allows the expression to be simplified to

$$[GeO(C_2O_4)_2^{2-}] = \frac{k_5'[Ge(C_2O_4)_3^{2-}]}{\{k_{-5}[H^+] + k_{-6}\}[HC_2O_4^-]}$$

where k_5' equals $k_5[H_2O]$. The initial reaction rate is given by

$$R = k_8[GeO(C_2O_4)_2^{2-}][HC_2O_4^-]^* = k_8k_7[GeO(C_2O_4)_2^{2-}][HC_2O_4^-]I$$

that leads to the final result

$$R = \frac{k_8k_7k_5'[Ge(C_2O_4)_3^{2-}]I}{k_{-5}[H^+] + k_{-6}} = \frac{\frac{k_8k_7k_5'}{k_{-5}}[Ge(C_2O_4)_3^{2-}]I}{[H^+] + k_{-6}/k_{-5}} = \frac{k'[X]I}{[H^+] + k''}$$

on substituting the expression for the $GeO(C_2O_4)_2^{2-}$ species.

It is possible that the ion $GeO(C_2O_4)_2^{2-}$ is primarily photoactivatable.

$$GeO(C_2O_4)_2^{2-} \xrightarrow{h\nu} [GeO(C_2O_4)_2^{2-}]^* \quad (10)$$

The photoactivated species participate in reaction (11) to produce a double activated species in which the two activated oxalate ligands are ring-opened. This intermediate decomposes according to reaction (12) into the reaction products.

$$[GeO(C_2O_4)_2^{2-}]^* + [HC_2O_4^-]^* \rightarrow GeO(C_2O_4)(C_2O_4^*)(HC_2O_4^*)^{3-} \quad (11)$$

$$GeO(C_2O_4)(C_2O_4^*)(HC_2O_4^*)^{3-} \rightarrow Ge(C_2O_4)_2^{2-} + 2CO_2 + OH^- \quad (12)$$

The addition of reactions (10), (11) and (12) to the suggested mechanism does not alter the obtained theoretical rate expression.

The expression

$$k_{II} = k_o - k_I = k_o - \frac{k'I}{[H^+] + k''}$$

for the rate constant of the thermal reverse reaction simplifies to

$$k_{II} = \frac{k_o[H^+] + k'''}{[H^+] + k''}$$

by assuming the irradiation intensity I to be a constant. The suggestion of a mechanism that obeys this rate-law is impossible unless more data concerning the behaviour of the germanium(II) photolysis product is available.

Acknowledgement

The authors gratefully acknowledge financial support from the S.A. Council for Scientific and Industrial Research and the S.A. Atomic Energy Board.

References

1 C. A. Parker, *Trans. Far. Soc., 50,* 1213 (1954); C. A. Parker and C. G. Hatchard, *J. Phys. Chem., 63,* 22 (1959); J. A. van den Berg, *J.S. African Chem. Inst., 22,* 12 (1969).
2 J. A. van den Berg and P. Scheiner, *J.S. African Chem. Inst., 21,* 113 (1968).
3 D. J. A. de Waal and J. A. van den Berg, *Tydskrif vir Natuurwetenskappe, 9,* 1 (1969).
4 E. L. J. Breet and R. van Eldik, Part I, *Inorg. Chim. Acta, 9,* 177 (1974).
5 R. van Eldik, *J.S. African Chem. Inst., 24,* 13 (1971).
6 R. van Eldik and J. A. van den Berg, *J.S. African Chem. Inst., 22,* 19 (1969).
7 F. Glockling, "The Chemistry of Germanium", Academic Press, London, 1969, p. 30.